SURFACE AZIMUTHAL ANCHORING ENERGY BETWEEN THE GRATING SURFACE AND NEMATIC LIQUID CRYSTAL LAYER STUDIED BY USING A GEOMETRIC MODEL

Chin-Lung Lin and Tei-Chen Chen
Department of Mechanical Engineering, National Cheng Kung University, Tainan, Taiwan, R.O.C.
E-mail: n1891121@mail.ncku.edu.tw; ctcx831@mail.ncku.edu.tw

Received October 2016, Accepted December 2016
No. 16-CSME-117, E.I.C. Accession 4003

ABSTRACT

A simple geometric model is proposed for estimating the azimuthal anchoring energy between the sinusoidal relief grating surface and nematic liquid crystal layer of a liquid crystal display (LCD) device as a function of the grating height and grating pitch. The model parameters are determined experimentally, and the model is then used to predict the surface azimuthal anchoring energy for gratings with various pitches and heights. It is shown that a good agreement exists between the predicted results for the surface azimuthal anchoring energy and the experimental data. Moreover, a good agreement is also observed between the estimated results and those obtained from Berreman's expression and finite element method (FEM) simulations, respectively. Overall, the experimental and numerical results show that for the nematic liquid crystal considered in the present study (4-n-pentyl-4'-cyanobiphenyl (5CB)), the surface azimuthal anchoring energy increases with an increasing grating height or a reducing grating pitch.

Keywords: liquid crystal; azimuthal anchoring energy; grating surface; Berreman's theory; surface topography; geometric model.

ÉNERGIE D'ANCRAGE AZIMUTHALE DE SURFACE ENTRE LA SURFACE DE GRATISSAGE ET LA COUCHE DE CRISTAUX LIQUIDE NEMATIQUE ÉTUDIÉE PAR UN MODÈLE GEOMÉTRIQUE

RÉSUMÉ

Un modèle géométrique simple est proposé pour estimer l'énergie d'ancrage azimutal entre la surface de réseau de relief sinusoïdal et la couche de cristal liquide nématique d'un dispositif d'affichage à cristaux liquides (LCD) en fonction de la hauteur de grille et du pas de grille. Les paramètres du modèle sont déterminés expérimentalement et le modèle est ensuite utilisé pour prédire l'énergie d'ancrage azimutal de surface pour des réseaux à différents emplacements et hauteurs. Il est démontré qu'il existe un bon accord entre les résultats prédits pour l'énergie d'ancrage azimutal de surface et les données expérimentales. De plus, un bon accord est également observé entre les résultats estimés et ceux obtenus à partir de l'expression de Berreman et de la méthode des éléments finis (FEM), respectivement. Dans l'ensemble, les résultats expérimentaux et numériques montrent que pour le cristal liquide nématique considéré dans la présente étude (4-n-pentyl-4'-cyanobiphényle (5CB)), l'énergie d'ancrage azimutal de surface augmente avec une hauteur de réseau croissante ou un réseau de réduction de pas.

Mots-clés : cristal liquide; énergie d'ancrage azimutal; surface de réseau; théorie de Berreman; topographie de surface; modèle géométrique.

1. INTRODUCTION

The periodical grating structure in liquid crystal displays (LCDs) is traditionally fabricated by applying a unidirectional mechanical rubbing process to a polymer-coated substrate using a velvet cloth. However, the rubbing process not only creates scrap, but also an electrostatic charge, which adversely affects the alignment of the liquid crystals. Accordingly, various alternative techniques for fabricating the crystal alignment layer have been proposed [1–9]. For example, Newsome et al. [1] used a laser ablation technique to pattern grating structures on a polymer layer. Scharf et al. [2] and Chiou et al. [3] used soft embossing techniques to fabricate nano- and micro-structured surfaces for liquid crystal alignment. Lin et al. [4] prepared U-shaped grooves with a variety of depths and periods on glass substrates using a reactive ion etching method. Hah et al. [5] used an imprinting technique to fabricate crystal alignment layers with square-, V- and U-shaped grooves, respectively. Hlaing et al. [6] utilized nanoimprinted structures to control both the morphology and the molecular chain orientation of thin-film conjugated polymers. Chiu et al. [7] proposed a method for fabricating polyimide micro/nano-structures using contact-transfer and mask-embedded lithography techniques. Gear et al. [8] demonstrated that patterned nanogrooves using electron beam lithography can be used to control the magnitude of the azimuthal anchoring energy of liquid crystals. Kim et al. [9] reported the fabrication of nanogrooves having sub-200-nm scale and the entire process can be completed in less than 30 minutes. In general, the results presented in [1–9] indicate that the molecular orientation of liquid crystals is significantly dependent on the shape of the grating pattern.

The surface azimuthal anchoring energy is one of the most important factors in characterizing the surface orientation of liquid crystal molecules [10]. The azimuthal anchoring energy of nematic liquid crystals is traditionally described using Berreman's model [11], which attributes the surface anchoring energy to the elastic distortion of the liquid crystals as a result of the grating structure. However, experimental studies have shown that while the Berreman's model yields accurate estimates of the anchoring energy for shallow-amplitude gratings, the results obtained for deep-amplitude gratings are less satisfactory [12]. Accordingly, an alternative model is required for obtaining accurate estimates of the azimuthal anchoring energy for both shallow- and deep-amplitude gratings.

To satisfy this requirement, the present study proposes a simple geometric model for predicting the azimuthal anchoring energy of nematic liquid crystals on a sinusoidal relief grating surface as a function of the grating height and the grating pitch. It is shown that the results obtained using the proposed model are in good agreement not only with the experimental data [13], but also with those obtained from the Berreman's model and finite element method (FEM) simulations [13, 14], respectively. In addition, it is shown that the surface azimuthal anchoring energy of the nematic liquid crystal considered in the present study (4-n-pentyl-4'-cyanobiphenyl (5CB) [15] with the chemical formula $C_{18}H_{19}N$) increases as the grating height increases and the grating pitch reduces.

2. THEORETICAL MODEL

The model proposed in this study for predicting the surface azimuthal anchoring energy of liquid crystals on a grating surface is derived from that for a microfluidic capillary-driven valve since the two cases have good structural similarity. In microfluidic capillary-driven valves [16–19], the fluid is blocked by a capillary stop valve with the form of an abrupt contraction or expansion of the channel. Man et al. [16] predicted the pressure barrier induced by a capillary stop valve using two-dimensional (2-D) meniscus analyses. Leu and Chang [17] obtained improved estimates of the pressure barrier by replacing the 2-D model with a modified three-dimensional (3-D) meniscus model. In the present study, the surface azimuthal anchoring energy is determined using a total interfacial energy formula based on a similar 3-D model. As shown in Fig. 1, the model considers a liquid-solid-gas interface system, and hence the total interfacial energy, U_T, can be written as

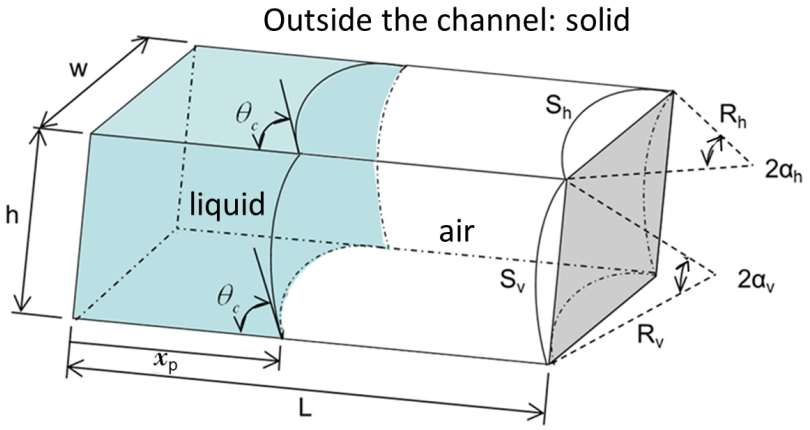

Fig. 1. Schematic illustration of the 3-D model.

$$U_T = A_{sl}\gamma_{sl} + A_{sa}\gamma_{sa} + A_{la}\gamma_{la}, \tag{1}$$

where A_{sl},A_{sa} and A_{la} are the solid-liquid, solid-air, and liquid-air interface areas, respectively. In addition, γ_{sl}, γ_{sa} and γ_{la} are the corresponding surface tension forces per unit length and are related to the equilibrium contact angle θ_c by the Young's equation, i.e.,

$$\gamma_{sa} = \gamma_{sl} + \gamma_{la}\cos\theta_c. \tag{2}$$

Substituting γ_{sl} shown in Eq. (2) into Eq. (1) yields

$$\begin{aligned} U_T &= (A_{sl} + A_{sa})\gamma_{sa} - A_{sl}\gamma_{la}\cos\theta_c + A_{la}\gamma_{la} \\ &= U_0 - A_{sl}\gamma_{la}\cos\theta_c + A_{la}\gamma_{la}, \end{aligned} \tag{3}$$

where $U_0 = (A_{sl} + A_{sa})\gamma_{sa}$ and its value remains invariant.

As shown in Fig. 1, the main design parameters of the 3-D model include: (a) the channel height, h; (b) the channel width, w; (c) the channel length, L; (d) the radii of curvature, R_h and R_v; (e) the arc lengths, S_h and S_v; and (f) the circular arc angles, i.e., $2\alpha_h(\alpha_h = \pi/2 - \theta_c)$ in the horizontal direction and $2\alpha_v(\alpha_v = \pi/2 - \theta_c)$ in the vertical direction. From basic geometric principles, the solid-liquid and liquid-air interface areas, A_{sl} and A_{la}, can be expressed, respectively, as

$$A_{sl} = 2x_p(w+h) - \frac{w^2}{2\sin\alpha_h}\left(\frac{\alpha_h}{\sin\alpha_h} - \cos\alpha_h\right) - \frac{h^2}{2\sin\alpha_v}\left(\frac{\alpha_v}{\sin\alpha_v} - \cos\alpha_v\right), \tag{4}$$

and

$$A_{la} \approx S_h \times S_v = 2\alpha_h R_h \times 2\alpha_v R_v = \left(\frac{\alpha_h w}{\sin\alpha_h}\right)\left(\frac{\alpha_v h}{\sin\alpha_v}\right). \tag{5}$$

In addition, the liquid volume, V_l, can be approximated as

$$V_l \approx whx_p - \frac{w^2 h}{4\sin\alpha_h}\left(\frac{\alpha_h}{\sin\alpha_h} - \cos\alpha_h\right) - \frac{h^2 w}{4\sin\alpha_v}\left(\frac{\alpha_v}{\sin\alpha_v} - \cos\alpha_v\right), \tag{6}$$

where x_p denotes the penetration distance.

As shown in Eq. (3), the total interfacial energy, U_T, is a function of the liquid volume, V_l. The effective pressure P applied on the fluid channel is given by the derivative of the total interfacial energy of the system with respect to the liquid volume V_l, i.e.,

$$P = -\frac{dU_T}{dV_l} = \gamma_{la}\left(\cos\theta_c \frac{dA_{sl}}{dV_l} - \frac{dA_{la}}{dV_l}\right) = \frac{2(w+h)\gamma_{la}\cos\theta_c}{wh}. \tag{7}$$

For a uniform channel, A_{la} is fixed and A_{sl} increases linearly with an increasing penetration distance. When the entire channel is full of liquid, the liquid volume, V_l, is equal to whL and the total interfacial energy is thus given as

$$U_T^* = P \times whL = 2L(w+h)\gamma_{la}\cos\theta_c = A_c(\gamma_{la}\cos\theta_c), \tag{8}$$

where A_c is the total solid-liquid interface area.

Wenzel [20] showed that for a rough surface, the contact angle is related to the equilibrium contact angle θ_c as follows

$$\cos\theta_c^* = r\cos\theta_c, \tag{9}$$

where θ_c^* and r are the apparent contact angle of the rough surface and the roughness factor, respectively. Note that the roughness factor is defined as the ratio of the actual surface to the geometric surface. For real solids, the actual surface is greater than the geometric surface due to surface roughness, and hence the roughness factor, r, has a value greater than unity. Consequently, Eq. (8) can be modified as

$$U_T^* = A_c(\gamma_{la}\cos\theta_c^*) = A_c(\gamma_{la} r\cos\theta_c), \tag{10}$$

For the liquid crystal cell considered in the present study, the grating surface is assumed to have a sinusoidal relief profile, as shown in Fig. 2. According to Berreman's theory, the surface profile can simply be modeled as

$$\xi(y) = \frac{H}{2}\sin\left(\frac{2\pi}{\lambda}y\right), \tag{11}$$

where H and λ are the grating height and grating pitch, respectively. The grating is assumed to have a uniform cross-sectional area along the x-direction on the y-z plane. Furthermore, the grating has a length L in the x-direction and is periodically distributed with n (number) pitches. From Eq. (10), the total interfacial energy can be obtained as

$$U_T^* = A_c(\gamma_{la} r\cos\theta_c) = L[n(\lambda + L_\sim) + 2d + H]\gamma_{la} r\cos\theta_c, \tag{12}$$

where d and $L_\sim$ are the cell gap and sinusoidal path length of each pitch of the grating, respectively. Note that the values of $L_\sim$ can be calculated directly using Eq. (11).

The surface azimuthal anchoring energy W_ϕ of the structure shown in Fig. 2 can be calculated as

$$k_p W_\phi = \frac{U_T^* - U_{\text{non}}}{A_s}, \tag{13}$$

where k_p is a proportional error parameter; U_{non} is the energy with no contribution to the surface azimuthal anchoring energy; and A_s is the total surface area of the liquid crystal cell structure. Rearranging Eq. (13) gives

$$U_T^* = k_p W_\phi A_s + U_{\text{non}}. \tag{14}$$

Substituting Eq. (12) into Eq. (14) yields

$$L[n(\lambda + L_\sim) + 2d + H]\gamma_{la} r\cos\theta_c = k_p W_\phi (n\lambda L) + U_{\text{non}}. \tag{15}$$

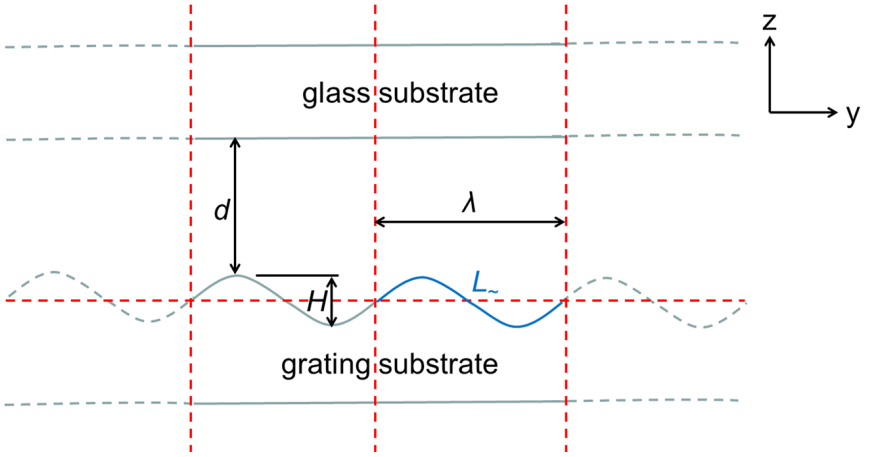

Fig. 2. Schematic illustration of liquid crystal cell structure with sinusoidal relief grating surface.

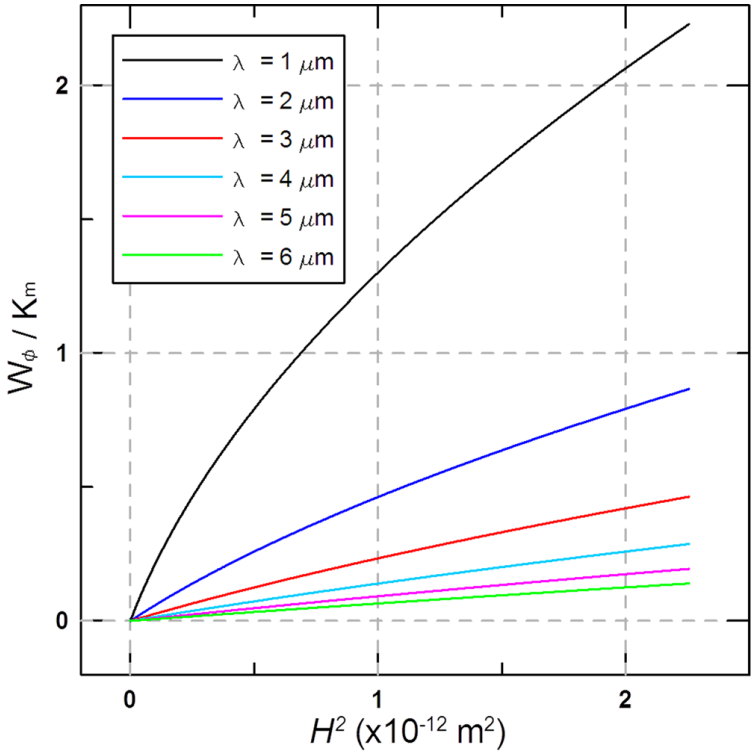

Fig. 3. Variation of W_ϕ/k_m with square of grating height for various values of grating pitch.

Dividing Eq. (15) by $k_p nL$ gives

$$(\lambda + L_\sim)k_m = W_\phi \lambda + U^*, \tag{16}$$

where

$$k_m = \frac{\gamma_{la} r \cos\theta_c}{k_p} \quad \text{and}$$

$$U^* = \frac{U_{\text{non}} - (2d+H)L\gamma_{la} r \cos\theta_c}{k_p nL}.$$

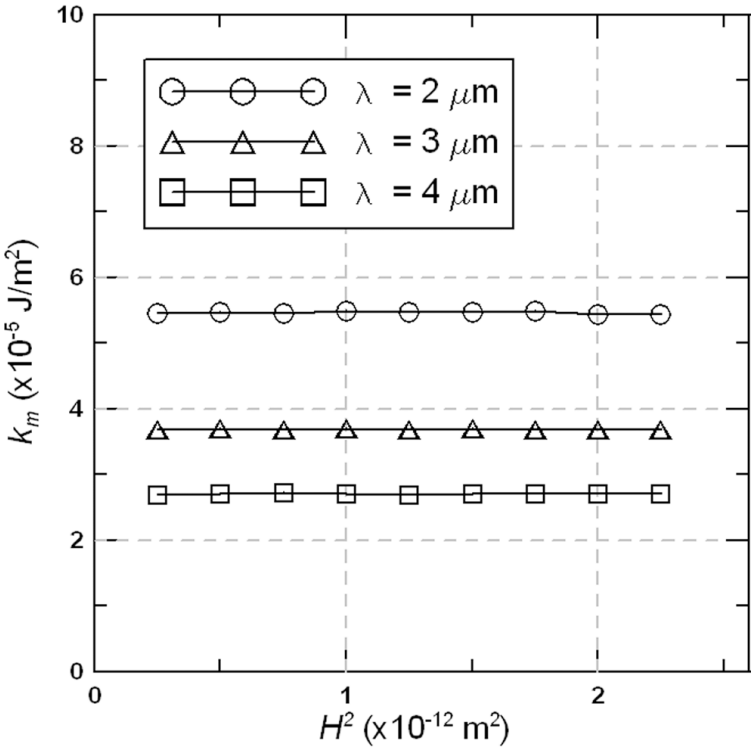

Fig. 4. Variation of k_m with square of grating height for various values of grating pitch.

For $L_\sim = \lambda, W_\phi = 0$. Therefore,

$$U^* = 2\lambda k_m. \tag{17}$$

Finally, substituting Eq. (17) into Eq. (16), the surface azimuthal anchoring energy can be obtained

$$W_\phi = \frac{L_\sim - \lambda}{\lambda} k_m = \left(\frac{L_\sim}{\lambda} - 1\right) k_m. \tag{18}$$

In other words, the geometric model for the surface azimuthal anchoring energy comprises three parameters, namely $L_\sim$ (the sinusoidal path length of each pitch), λ (the grating pitch), and k_m (major factor).

3. RESULTS AND DISCUSSION

Figure 3 plots the results obtained from the geometric model (Eq. (18)) for the variation of W_ϕ/k_m with the square of the grating height for various values of the grating pitch λ in the range of 1–6 μm. For each value of the grating pitch, W_ϕ/k_m increases almost linearly with increasing H^2. In other words, the results are consistent with those obtained by FEM simulations in [13, 14], and hence the basic validity of the proposed model is confirmed.

In implementing the geometric model, parameter k_m was firstly determined from Eq. (18) using the FEM data [13]. The results presented in Fig. 4 show that for a given value of the grating pitch, k_m remains approximately constant as H^2 increases. However, for a given grating height, k_m reduces with an increasing grating pitch. From inspection, the average values of k_m for grating pitches of 2, 3 and 4 μm are $5.464 \times 10^{-5}, 3.687 \times 10^{-5}$, and 2.702×10^{-5} J/m^2, respectively.

The validity of the proposed geometric model was demonstrated by comparing the results obtained for the azimuthal anchoring energy of 4-*n*-pentyl-4'-cyanobiphenyl (5CB) nematic liquid crystal with the experimental data presented in [13] for grating structures fabricated using a photoresist technique with three

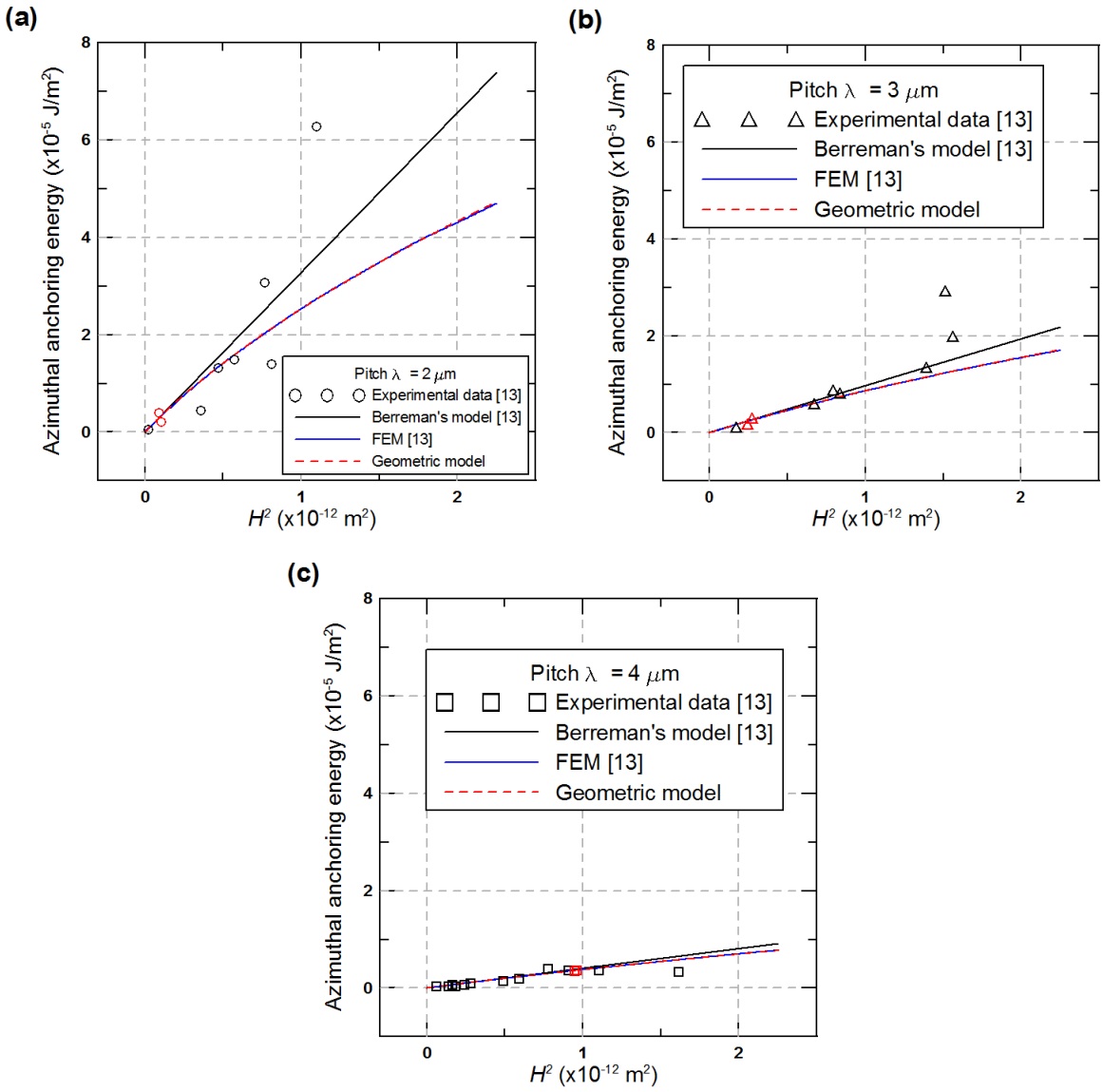

Fig. 5. Experimental and numerical results for variation of surface azimuthal anchoring energy with square of grating height for grating pitches of: (a) $\lambda = 2$ μm, (b) $\lambda = 3$ μm, and (c) $\lambda = 4$ μm.

different pitch sizes, namely 2, 3 and 4 μm. In fabricating the grating structures, the grating height was controlled by adjusting the intensity of the UV laser beam. Following UV exposure, the average grating height was measured using an atomic force microscope. Liquid crystal cells with a gap size of 25 μm were then fabricated by combining the grating substrates with a second glass substrate on which polyvinyl alcohol (PVA) was coated and pre-rubbed.

Figures 5a–5c show the experimental results obtained for the variation of the azimuthal anchoring energy with the square of the grating height for the grating structures with pitches of $\lambda = 2, 3$ and 4 μm, respectively. It is seen that for each value of the grating pitch, some pairs of data points (open symbols) overlap at certain values of the squared grating height. Intuitively, a greater degree of overlap implies a smaller experimental error. Thus, for each value of λ, the average value of the closest overlapping data points (red symbols) was used to determine the corresponding value of k_m using Eq. (18). The values of k_m were found to be in good

agreement with those obtained via FEM simulations in Fig. 4. Having determined the value of k_m for each grating pitch, the geometric model (Eq. (18)) was used to compute the variation of the azimuthal anchoring energy with the square of the grating height over the range of $H^2 = 0 \sim 2.25 \times 10^{-12}$ m^2. The corresponding results are shown by the red dashed lines in Fig. 5.

For comparison purposes, the azimuthal anchoring energy was also evaluated using the Berreman's model and FEM simulations, respectively. According to Berreman's model [11, 13, 14], the azimuthal anchoring energy can be estimated as

$$W_\phi = \frac{1}{2} K \left(\frac{H}{2}\right)^2 \left(\frac{2\pi}{\lambda}\right)^3, \tag{19}$$

where K is the mean of the splay and bend elastic constants of the liquid crystal (8.47×10^{-12} N for the 5CB nematic liquid crystal considered in the present study). The corresponding results are shown by the solid black lines in Fig. 5. In [13, 14], the authors evaluated the azimuthal anchoring energy by means of FEM simulations based on a 2-D model and an elastic energy minimization principle. The corresponding results are shown by the solid blue lines in Fig. 5.

As shown in Fig. 5, a saturation tendency of the surface azimuthal anchoring energy is observed as the square of the grating height increases for all three calculation methods (i.e., Berreman's model, FEM simulations and geometric model). In addition, a good agreement exists between the three sets of numerical results and the experimental data for shallow grating structures (i.e., $H^2 < 0.5 \times 10^{-12}$ m^2). However, for deeper grating structures (i.e., $H^2 > 0.5 \times 10^{-12}$ m^2), the surface azimuthal anchoring energy values obtained using Berreman's model are greater than those obtained from the FEM simulations or geometric model. In other words, the results confirm that Berreman's model is more applicable to shallow-amplitude grating structures [12].

As shown in Fig. 5, a good agreement exists between the FEM results and those obtained from the proposed geometric model for all values of the grating pitch and grating height. In other words, the FEM results can be used to determine parameter k_m for a given grating pitch and k_m can then be used in the geometric model to predict the surface azimuthal anchoring energies for any required grating height. That is, the two methods can be combined to form a new approach for predicting the surface azimuthal anchoring energy for grating structures with various heights and pitches.

Overall, the results presented in Fig. 5 show that for the 5CB nematic liquid crystal considered in the present study, the surface azimuthal anchoring energy increases with an increasing grating height (i.e., square of grating height) given a constant grating pitch. By contrast, for a given grating height, the azimuthal anchoring energy increases with a decreasing grating pitch.

4. CONCLUSIONS

A simple geometric model has been proposed for estimating the azimuthal anchoring energy between the sinusoidal relief grating surface and nematic liquid crystal layer of a LCD device as a function of the grating height and grating pitch. The proposed model is based on three parameters, namely $L_\sim$ (the sinusoidal path length of each pitch), λ (the grating pitch), and k_m (major factor), where the latter parameter is determined directly from experimental or FEM data. The validity of the proposed model has been confirmed by comparing the results obtained for the azimuthal anchoring energy with those obtained experimentally and by the Berreman's model and FEM simulations, respectively. A good agreement has been observed between all three methods and the experimental results for shallow-amplitude gratings. For deeper-amplitude gratings, the Berreman's model overstates the azimuthal anchoring energy. However, a good agreement is observed between the results obtained using the proposed geometric model and those obtained from FEM simulations. Finally, it has been shown that for 5CB nematic liquid crystal, the surface azimuthal anchoring energy increases with an increasing grating height or a reducing grating pitch.

Overall, the saturation tendency of the anchoring energy with an increasing grating height is successfully predicted by both FEM simulations and the proposed geometric model. However, the geometric model is more easily implemented than FEM simulations. Moreover, the results which obtained using the geometric model are in good agreement with the experimental data. Thus, the two methods can be combined to realize a simple yet accurate means of predicting the anchoring properties of grating surfaces with any given values of the grating pitch and grating height.

ACKNOWLEDGEMENT

The authors would like to thank the Ministry of Science and Technology of the Republic of China, Taiwan, for the financial support of this study under Contract No. MOST 105-2221-E-006-079-.

REFERENCES

1. Newsome, C.J., O'Neill, M., Farley, R.J. and Bryan-Brown, G.P., "Laser etched gratings on polymer layers for alignment of liquid crystals", *Applied Physics Letters*, Vol. 72, No. 17, pp. 2078–2080, 1998.
2. Scharf, T., Shlayen, A., Gernez, C., Basturk, N. and Grupp, J., "Liquid crystal alignment on replicated nanostructured surfaces", *Molecular Crystals and Liquid Crystals*, Vol. 412, No. 1, pp. 135–145, 2004.
3. Chiou, D.-R., Chen, L.-J. and Lee, C.-D, "Pretilt angle of liquid crystals and liquid-crystal alignment on microgrooved polyimide surfaces fabricated by soft embossing method", *Langmuir*, Vol. 22, No. 22, pp. 9403–9408, 2006.
4. Lin, Y.-F., Tsou, M.-C. and Pan, R.-P, "Alignment of liquid crystals by ion etched grooved glass surfaces", *Chinese Journal of Physics*, Vol. 43, No. 6, pp. 1066–073, 2005.
5. Hah, H., Sung, S.-J., Han, M., Lee, S. and Park, J.-K., "Effect of the shape of imprinted alignment layer on the molecular orientation of liquid crystal", *Materials Science and Engineering: C*, Vol. 27, No. 4, pp. 798–801, 2007.
6. Hlaing, H., Lu, X., Hofmann, T., Yager, K.G., Black, C.T. and Ocko, B.M., "Nanoimprint-induced molecular orientation in semiconducting polymer nanostructures", *ACS Nano*, Vol. 5, No. 9, pp. 7532–7538, 2011.
7. Chiu, C.-Y. and Lee, Y.-C., "Fabrication of polyimide micro/nano-structures based on contact-transfer and mask-embedded lithography", *Journal of Micromechanics and Microengineering*, Vol. 19, No. 10, pp. 105001, 2009.
8. Gear, C., Diest, K., Liberman, V., and Rothschild, M., "Engineered liquid crystal anchoring energies with nanopatterned surfaces", *Optics Express*, Vol. 23, No. 2, pp. 807–814, 2015.
9. Kim, D.S., Cha, Y.J., Gim, M.-J., and Yoon, D.K., "Fast fabrication of sub-200-nm nanogrooves using liquid crystal material", *ACS Applied Materials & Interfaces*, Vol. 8, No. 18, pp. 11851–11856, 2016.
10. Dadivanyan, A.K., Noah, O.V., Pashinina, Yu.M., Belyaev, V.V., Chigrinov, V.G. and Chausov, D.N., "Anchoring energy of liquid crystals", *Molecular Crystals and Liquid Crystals*, Vol. 560, No. 1, pp. 108–114, 2012.
11. Berreman, D.W., "Solid surface shape and the alignment of an adjacent nematic liquid crystal", *Physical Review Letters*, Vol. 28, No. 26, pp. 1683–1686, 1972.
12. Hallam, B.T. and Sambles, J.R., "Groove depth dependence of the anchoring strength of a zero order grating-aligned liquid crystal", *Liquid Crystals*, Vol. 27, No. 9, pp. 1207–1211, 2000.
13. Kimura, M., Ohta, Y. and Akahane, T., "Surface azimuthal anchoring energy between the trapezoid grating surface and nematic liquid crystal layer studied by finite element method", *Advances in Technology of Materials and Materials Processing Journal*, Vol. 7, No. 2, pp. 91–96, 2005.
14. Ohta, Y., Tanaka, N., Kimura, M. and Akahane, T., "Surface azimuthal anchoring energy between the grating surface and nematic liquid crystal layer by finite element method", *Japanese Journal of Applied Physics*, Vol. 43, No. 7A, pp. 4310–4311, 2004.
15. Gray, G.W., Harrison, K.J., Nash, J.A., "New family of nematic liquid crystals for displays", *Electronics Letters*, Vol. 9, No. 6, pp. 130–131, 1973.
16. Man, P.F., Mastrangelo, C.H., Burns, M.A. and Burke, D.T., "Microfabricated capillarity-driven stop valve and sample injector", in *Proceedings of the IEEE MEMS'98*, Heidelberg, Germany, pp. 45–50, January 25–29, 1998.
17. Leu, T.-S. and Chang, P.-Y., "Pressure barrier of capillary stop valves in micro sample separators", *Sensors and Actuators A: Physical*, Vol. 115, No. 2–3, pp. 508–515, 2004.

18. Duffy, D.C., Gillis, H.L., Lin, J., Sheppard, N.F., Jr. and Kellogg, G.J., "Microfabricated centrifugal microfluidic systems: characterization and multiple enzymatic assays", *Analytical Chemistry*, Vol. 71, No. 20, pp. 4669–4678, 1999.
19. Fu, B.-R., "Liquid-liquid mixtures flow in microchannels", *Transactions of the Canadian Society for Mechanical Engineering*, Vol. 37, No. 3, pp. 631–640, 2013.
20. Wenzel, R.N., "Resistance of solid surfaces to wetting by water", *Industrial & Engineering Chemistry*, Vol. 28, No. 8, pp. 988–994, 1936.